

Liquefaction Potential Mapping in Memphis and Shelby County, Tennessee

Glenn J. Rix¹ and Salome Romero-Hudock¹

The Earthquake Hazards Program of the U.S. Geological Survey is developing seismic hazard maps for several urban areas in the United States including Memphis and Shelby County, Tennessee. In this study, liquefaction hazard maps are developed for six, 7.5-minute quadrangles in the Memphis and Shelby County area using available standard penetration test (SPT) and cone penetration test (CPT) data. For each SPT and CPT profile, the liquefaction potential index (LPI) is calculated as a function of seismic demand, and the results are aggregated based on surface geology. This yields the probability of moderate ($LPI > 5$) and major ($LPI > 15$) liquefaction in each geological unit as a function of seismic demand. Subsequently, liquefaction hazard maps are prepared for a $M_w = 7.7$ scenario earthquake and expected ground motions in the study area. The maps indicate that Holocene alluvial deposits associated with floodplains of major rivers in the area have the greatest potential for liquefaction.

INTRODUCTION

The City of Memphis, Tennessee and surrounding Shelby County constitute a large, urban area that is prone to damage from earthquakes in the New Madrid Seismic Zone (NMSZ), which extends from southeastern Missouri to northwestern Tennessee and northeastern Arkansas and generated three large events in 1811-1812. Best estimates of the moment magnitudes for the three events range from 7.5 to 7.8 (Bakun and Hopper, 2004). The recurrence interval for events of this size is estimated to be 500 years \pm 300 years based on geologic data from the 1811-1812 and previous earthquake sequences (Tuttle et al., 2002).

Memphis and Shelby County are located within the Upper Mississippi Embayment, a southward plunging trough that extends from southern Illinois to the Gulf of Mexico. Embayment deposits are composed of unconsolidated sediments from the post-Paleozoic period ranging in thickness from a few meters along the edges of the embayment to more than 1000 m along the axis of the embayment. Surficial deposits in the Memphis and Shelby County area (see Figure 1) include Holocene artificial fill, Holocene alluvial deposits along river channels, Pleistocene loess and terrace deposits in interfluvial regions, and Pliocene-

¹ Georgia Institute of Technology, School of Civil and Environmental Engineering, Atlanta, GA 30332

Pleistocene Upland deposits known as the Lafayette gravel (Broughton et al., 2001). Table 1 provides more detailed information on the composition of each unit. The Mississippi River borders Memphis and Shelby County along the west. The Wolf River runs east to west through the northern half of the study area and flows into the Mississippi River near Mud Island, which originated as a sand bar in the Mississippi River (Clay, 1986) and has been developed in recent years. The alluvial floodplains of the Wolf River and the Mississippi River are composed of Holocene-age deposits. Nonconnah Creek runs east to west through the southern half of the study area, and its floodplain is composed of reworked loess. Artificial fill is subjectively defined and mapped in the region (Gomberg, 2004) and includes both engineered fills and non-engineered fills. The map does not distinguish between the two types.

Many of these deposits are susceptible to liquefaction. Liquefaction features caused by the 1811-1812 earthquakes as well as earthquakes in approximately 900 A.D. and 1450 A.D. have been mapped throughout the Upper Mississippi Embayment (Obermeier, 1989; Tuttle et al., 2002) and as yet undated features along the Wolf and Loosahatchie Rivers in Memphis and Shelby County (Broughton et al., 2001). Liquefaction susceptibility maps have previously been developed for the Memphis and Shelby County region based on the type and age of geologic deposits (Broughton et al., 2001; Van Arsdale and Cox, 2003) using the methodology proposed by Youd and Perkins (1978). Liquefaction susceptibility maps have also been developed using a simple classification scheme based on standard penetration tests (SPT) (Lin et al., 1996; Hwang et al., 1999). The effect of human activities on liquefaction hazards has been considered by Yates et al. (2003) who documented aggradation and denudation along the Wolf River floodplain since the 1940s and suggest that these changes may increase the susceptibility to liquefaction and severity of lateral spreading.

These previous studies focused on the susceptibility of geologic deposits to liquefaction and did not consider the seismic demand required to initiate liquefaction or the severity of liquefaction. In this study, liquefaction *potential* maps are developed for six, 7.5-minute quadrangles (Northwest Memphis, Northeast Memphis, Southwest Memphis, Southeast Memphis, Ellendale, and Germantown) in the Memphis and Shelby County area (see Figure 1). Seismic demand is obtained from a complementary study by Cramer et al. (2004) that estimated ground motions in the study area. Liquefaction resistance is derived from available standard penetration test (SPT) and cone penetration test (CPT) profiles. For each profile, the

factor of safety against liquefaction is determined using the “simplified procedure” (Seed and Idriss, 1971; Youd et al., 2001). The liquefaction potential index (LPI) (Iwasaki et al., 1978; 1982) is calculated for each profile based on the factor of safety against liquefaction. The LPI results are then aggregated according to the surficial geology. The liquefaction potential maps show the probability of “moderate” and “major” liquefaction as defined by Iwasaki et al. (1982) within each geologic unit for a given earthquake scenario. Because of the uncertainties regarding artificial fill noted above, fills are shown as areas that require site-specific studies. The methodology employed in this study is similar to that used by Holzer et al. (2002; 2006a) to develop liquefaction potential maps for the Oakland, CA area for scenario earthquakes on the Hayward Fault and by Holzer et al. (2006b) to predict the extent of liquefaction in East Bay fills due to a repeat of the 1906 San Francisco earthquake.

SIMPLIFIED PROCEDURE AND LIQUEFACTION POTENTIAL INDEX

The simplified procedure (Seed and Idriss, 1971) compares the seismic demand expressed in terms of the cyclic stress ratio to the liquefaction resistance of the soil represented by the cyclic resistance ratio. The cyclic stress ratio is proportional to the peak ground acceleration a_{\max} . The cyclic resistance ratio for a $M_w = 7.5$ earthquake ($CRR_{7.5}$) may be determined from the equivalent clean sand standard penetration resistance $(N_1)_{60cs}$ or from the equivalent clean sand normalized cone tip resistance $(q_{c1N})_{cs}$ (Youd et al., 2001). A magnitude scaling factor (also called a magnitude-correlated duration weighting factor) is used to adjust $CRR_{7.5}$ for other magnitudes (Youd et al., 2001). The factor of safety against triggering of free-field, level ground liquefaction is defined as

$$FS = \frac{CRR_{7.5}}{CSR} MSF \quad (1)$$

where MSF is the magnitude scaling factor.

For subsequent analyses, it is convenient to represent the seismic demand with a single expression that captures the combined effects of peak ground acceleration and duration (via the magnitude scaling factor). Inspection of Equation 1 indicates that an appropriate expression is

$$\text{Demand} = \frac{CSR}{MSF} \propto \frac{a_{\max}}{MSF} \quad (2)$$

which may be viewed as a duration-adjusted peak ground acceleration.

The liquefaction potential maps developed herein are based on the liquefaction potential index (LPI) proposed by Iwasaki et al. (1978; 1982) and given by

$$LPI = \sum_{i=1}^n w_i S_i H_i \quad (4)$$

where n is the number of layers in the upper 20 m of the deposit, w is a depth-dependent weighting function, H is the thickness of each layer, and S is defined as

$$S = \begin{cases} 0 & \text{for } FS > 1 \\ 1 - FS & \text{for } FS < 1 \end{cases} \quad (5)$$

Iwasaki et al. (1982) identified LPI values of 5 and 15 as the lower bounds of “moderate” and “major” liquefaction, respectively, from SPT measurements at 85 Japanese sites subjected to six earthquakes. Toprak and Holzer (2003) found similar results using 50 CPT soundings at 20 sites affected by the 1989 Loma Prieta ($M_w = 6.9$) earthquake to correlate LPI with surface manifestations of liquefaction. Specifically, they found that median values of LPI equal to 5 and 12 corresponded to the occurrence of sand boils and lateral spreading, respectively. Analyses of liquefaction features from the 2003 $M_w = 6.5$ San Simeon earthquake also support the use of LPI=5 as the threshold for surface manifestations of liquefaction (Holzer et al., 2005). LPI is potentially of great use for spatial analysis of liquefaction hazards because it allows one to develop a two-dimensional representation of a three-dimensional phenomenon (i.e., FS vs. depth), which is ideal for mapping (Luna and Frost, 1998), and it correlates well with liquefaction effects (Toprak and Holzer, 2003).

PENETRATION TEST AND GROUNDWATER DATA

Liquefaction analyses were performed using 623 SPT profiles obtained from databases compiled by Ng et al. (1989) and Hwang et al. (1999). Figure 2a shows the location of the SPT data within the six quadrangles, and Table 2 summarizes the number of SPT profiles in each geologic unit. Although the SPT data are plentiful, they are often incomplete (i.e., profiles are less than 20 m deep and/or soil classification information is absent), and limited information is available regarding the hammer energy, fines content, and other parameters needed for liquefaction analysis.

Eighteen CPT profiles were obtained from five sites in the study area (Liao et al., 2001; 2002). Because of the small number of profiles, data from the adjacent Collierville quadrangle were also included. The locations of the CPT profiles are shown in Figure 2b, and Table 2 summarizes the number of profiles in each geologic unit. The CPT data are limited in number but high in quality. The Qal unit was not mapped using CPT data because of the absence of profiles in the unit.

The position of the groundwater table is an important parameter for liquefaction analysis. Hwang et al. (1999) provide the depth to groundwater for 464 wells in the Memphis area. The values range from 2 m to 13 m. For our analyses, we assumed a constant, median depth to the groundwater table of 6 m for the entire study area. We discuss the effect of this assumption on the calculated values of LPI subsequently.

LIQUEFACTION ANALYSIS USING SPT DATA

Liquefaction analyses using SPT data require information on the fines content of the soil and hammer energy ratio to correct the raw N_m values to an equivalent clean sand value, $(N_1)_{60cs}$. In this study, the Unified Soil Classification System (USCS) classification was used to estimate the fines content of the soil because grain size distribution data were not available. Table 3 lists the assumed fines content for coarse-grained soils, which corresponds to the minimum value for each soil type. This assumption is conservative because liquefaction resistance increases with fines content for a given value of N_m . Fine-grained soils were assumed to be non-liquefiable and were assigned a value of S equal to zero. The hammer energy ratio was assumed equal to 60% for all tests.

Incomplete SPT and/or Classification Data

As noted above, many of the SPT profiles were incomplete, lacking either SPT or soil classification data to the desired depth of 20 m. SPT profiles less than 15 m in depth were discarded. The remaining profiles were divided into the six categories listed in Table 4 based on the completeness of SPT and USCS information.

For SPT profiles less than 20 m in depth, the last measured standard penetration resistance (N_m) was extended to 20 m to complete the profile. This assumption was evaluated by eliminating data from a sample of the complete SPT profiles (Category 1) and replacing it with assumed values of N_m . The extrapolation of N_m below 15 m or 18 m does not strongly

affect the resulting LPI values. For profiles extrapolated below 18 m, the assumption produces no measurable difference. For profiles extrapolated below 15 m, the resulting values of LPI are slightly conservative, which is expected because N_m generally increases with depth.

Representative soil profiles (Figure 3) were developed for each geologic region based on the complete profiles available within the region. For SPT profiles with incomplete USCS information, the soil type from the representative profile at the corresponding depth was used.

LIQUEFACTION ANALYSIS USING CPT DATA

A consequence of the limited number of CPT profiles is that the heterogeneity (i.e., material variability) of the geologic unit is not likely to be captured accurately. Therefore, the measured CPT profiles were supplemented by stochastically simulated profiles in an effort to better represent the distribution of tip and sleeve resistance values within each unit. The simulated profiles are based on the measured CPT profiles in each geologic region. For each measured CPT profile, the cone tip resistance (q_t) profile was visually inspected and separated into layers with similar mean and variance. The lognormal mean ($\mu_{\log q_t}$) and the lognormal standard deviation ($\sigma_{\log q_t}$) were calculated for each layer. The standard normal residual value of q_t was calculated by

$$q_{norm} = \frac{\log q_t - \mu_{\log q_t}}{\sigma_{\log q_t}} \quad (7)$$

The spatial correlation between q_{norm} values within each sounding must be modeled to accurately simulate CPT profiles. An exponential autocorrelation function (ρ) defined by

$$\rho(h) = \exp\left(\frac{-3h}{a}\right) \quad (8)$$

models the experimental autocorrelation function obtained from the measured CPT q_t profiles where h is the spatial lag between depth measurements and a is the effective range over which the depth measurements are highly correlated (Deutsch and Journel, 1998).

The LU decomposition algorithm in the geostatistical software GSLIB (Deutsch and Journel 1998) was used to generate simulated q_t profiles based on the calculated values of lognormal mean, lognormal standard deviation, and effective range. The accompanying sleeve resistance (f_s) was simulated using a conditional probability density function since the sleeve resistance and cone tip resistance are correlated to soil type (e.g., Robertson, 1990). A total of 1200 simulated profiles of q_t and f_s were generated for each geologic region.

Another consequence of using a limited CPT data set is a likely bias in selection of sites. Many of the CPT tests were performed by Liao et al. (2001; 2002) to obtain geotechnical data at paleoliquefaction sites. As such, there may be a bias towards soils that are more susceptible to liquefaction.

SPT AND CPT RESULTS

The procedures described above were used to calculate the LPI for each SPT and CPT profile for a_{\max} values of 0.1 g, 0.2 g, 0.3 g, 0.4 g, and 0.5 g and M_w values of 6.0, 6.5, 7.0, 7.5, and 8.0 (i.e., 25 combinations of a_{\max} and M_w) to evaluate the distribution of LPI within each geologic unit for a range of seismic demands. Figure 4 shows examples of the histograms of the LPI for unit Qa, $a_{\max} = 0.3$ g, and $M_w = 8.0$. Using these LPI distributions, it is possible to calculate the probability of exceeding LPI values of 5 and 15, which we take as the lower bounds of “moderate” and “major” liquefaction, respectively, based on the results of Iwasaki et al. (1982) and Toprak and Holzer (2003). Figures 5 and 6 show the probability of exceeding LPI values of 5 and 15, respectively, as a function of the duration-adjusted peak ground acceleration for each geologic unit based on the SPT and CPT data.

The probability values may be interpreted in two ways. As an example, consider the probability of exceeding an LPI of 5 for unit Qa with $a_{\max} = 0.3$ g and $M_w = 8.0$ based on SPT data, which is approximately 50 percent. On one hand, we may say that the probability of moderate liquefaction at a particular site within the Qa unit is 50 percent. Alternatively, we may also say that 50 percent of the total area of the Qa unit is likely to experience moderate liquefaction. Holzer et al. (2006a) suggest that the former interpretation may be useful for engineering studies, while public officials and the general public may more readily understand the latter interpretation. Both interpretations require one to assume that the soil properties are statistically homogeneous within a given geologic unit. This assumption is

tenuous for the CPT-based analyses of the Ql and Qtl units because of the small number of profiles available for each unit.

In general, the CPT results exhibit a much more abrupt transition from lower to higher probabilities. This is a direct consequence of the limited number of CPT profiles and the inability to adequately capture the heterogeneity of soil properties within each unit. It is also interesting to note that the CPT results yield probabilities that are generally less than the SPT results. One possible interpretation is that the CPT results are less biased due to the inclusion of data from paleoliquefaction sites than originally believed.

INFLUENCE OF ASSUMED DEPTH TO GROUNDWATER TABLE

As noted previously, a median depth to groundwater of 6 m was assumed for the entire study area. This assumption was evaluated by comparing the LPI obtained for groundwater depths of 2 m, 4 m, 8 m, 10 m, and 12 m. Figure 7 shows the results as the ratio of the LPI for a particular assumed depth to the LPI for a depth of 6 m. The effect of the groundwater table decreases with increasing seismic demand. As expected, decreasing the depth to the groundwater table increases the liquefaction potential.

For groundwater depths ranging from 4 to 12 m and values of a_{\max}/MSF greater than 0.14, the error is generally less than 20 percent, which is considered acceptable for a regional study of this type. For values of a_{\max}/MSF less than 0.14, the errors associated with using an assumed groundwater depth of 6 m are potentially larger. However, the probabilities of moderate or major liquefaction (i.e., LPI values exceeding 5 and 15, respectively) are generally very low for these low seismic demands (Figures 5 and 6). As such, the practical consequences are limited. For shallow groundwater depths, represented here by an assumed depth of 2 m, the effects are more significant for all levels of seismic demand, and site-specific analyses are warranted.

LIQUEFACTION HAZARD MAPS FOR A $M_w = 7.7$ SCENARIO EARTHQUAKE

As an example of the use of this approach, we used seismic demand parameters provided by Cramer et al. (2004) to prepare liquefaction hazard maps for the study area. Cramer et al. used the same source and path parameters as the 2002 USGS National Seismic Hazard maps (Frankel et al., 2002) supplemented by site response analyses to incorporate the effects of the thick soil column underlying the Memphis and Shelby County area. The 2002 National Seismic Hazard Maps use a logic tree for the New Madrid Seismic Zone based on four

characteristic magnitudes (7.3, 7.5, 7.7, and 8.0) representing estimates of the 1811-1812 New Madrid earthquakes. Each magnitude is weighted according to the expected values of the 1811-1812 earthquakes (Wheeler and Perkins, 2000). The logic tree produces the same mean hazard as $M_w = 7.7$ (Frankel et al., 2002), and Cramer et al. (2004) used this magnitude to calculate scenario ground motions for the study area. Figure 8 shows the values of a_{max} , which range from 0.29 to 0.43 g. Interested readers should refer to Cramer et al. (2004) for additional information regarding the methods used to calculate ground motions in the study area.

Figures 9 and 10 show the corresponding liquefaction hazard maps, which give the probabilities of exceeding LPI values of 5 and 15, respectively, based on both SPT and CPT data. The probability values are binned in increments of 20 percent to better reflect the uncertainties in this approach.

Combined SPT and CPT Data

Combining the SPT and CPT results to obtain a single probability value for each unit requires a decision regarding the proper balance between results based on a large number of SPT profiles of uncertain quality and a small number of CPT profiles of high quality. For this example, we chose to assign a weight of two-thirds to the SPT data and one-third to the CPT data because we believe the more plentiful SPT data better captures the heterogeneity within each geologic unit. However, we readily admit that this choice was somewhat arbitrary and other combinations can be justified. Figure 11 shows the liquefaction hazard maps for moderate and major liquefaction due to a $M_w = 7.7$ scenario earthquake in the study area. Digital versions of these maps as well as those for a $M_w = 6.2$ scenario earthquake are available at the web site of the U.S. Geological Survey Earthquake Hazards Program.

Comparison with Paleoliquefaction Sites

As noted earlier, Broughton et al. (2001) found sand dikes along the Wolf and Loosahatchie Rivers that vary in width from 1 cm to 50 cm. The locations of the observed dikes are shown in Figure 11. Although none of the dikes were radiometrically dated, Broughton et al. indicate that they were likely formed during the 1811-1812 New Madrid earthquakes. Based on the spatial distribution and size of the dikes, Broughton et al. suggest that the Wolf River floodplain is the area most susceptible to liquefaction hazards within the study area. The probabilities of moderate and major liquefaction calculated in this study are

also the largest along the Wolf River and thus consistent with the findings of Broughton et al. (2001).

CONCLUSIONS

Liquefaction hazard maps for two scenario earthquakes have been prepared for six quadrangles in the Memphis and Shelby County, Tennessee area using the simplified procedure with available SPT and CPT profiles and the Liquefaction Potential Index to estimate the severity of liquefaction. SPT and CPT profiles were aggregated according to the surficial geology and were used to calculate the probability of exceeding threshold values of LPI corresponding to moderate and major liquefaction-induced ground failures as a function of the duration-adjusted peak ground acceleration. Probability values may be interpreted as the likelihood of a liquefaction-induced ground failure at a individual location or as the percentage of the geologic unit that is expected to experience liquefaction of a particular severity depending on the application and the audience.

In this study as well as those by Holzer and colleagues employing the same methods, the combination of the simplified procedure, Liquefaction Potential Index, and aggregation using surficial geology has been shown to be an effective approach for regional liquefaction hazard mapping. The primary uncertainties in this study are related to the low quality of the SPT data (i.e., profiles less than 20 m deep and missing soil classification, fines content, and hammer energy information) and the small number of high-quality CPT profiles. The hazard maps prepared for Memphis and Shelby County require deciding which of these two undesirable situations is the lesser evil. This limitation can be overcome by including resources to collect plentiful, high-quality penetration test data that adequately samples each surficial geologic unit in future applications of this method. The most important inherent limitation of the method itself is the need to assume that each geologic unit is statistically homogeneous.

Finally, it is important to recognize that the results of regional liquefaction hazard studies should not be construed as a replacement for site-specific analyses.

ACKNOWLEDGMENTS

The authors are grateful for the assistance provided by Dr. Chris Cramer, Dr. Joan Gomberg, Dr. Tom Holzer, and Dr. Eugene Schweig, all of the U.S. Geological Survey; Dr.

Roy Van Arsdale of the University of Memphis; and Dr. Scott Olson of the University of Illinois at Urbana-Champaign.

Research supported by the U.S. Geological Survey (USGS), Department of the Interior, under USGS award number Award No. 01-HQ-AG-0019. The views and conclusions contained in this document are those of the authors and should not be interpreted as necessarily representing the official policies, either expressed or implied, of the U.S. Government.

REFERENCES

- Bakun, W. H., and Hopper, M.G., 2004. Magnitudes and Locations of the 1811-1812 New Madrid, Missouri and the 1886 Charleston, South Carolina, Earthquakes, *Bulletin of the Seismological Society of America*, **94**(1), 64-75.
- Broughton, A.T., Van Arsdale, R.B., and Broughton, J.H., 2001. Liquefaction susceptibility mapping in the city of Memphis and Shelby County, Tennessee, *Engineering Geology* **62**, 201-222.
- Broughton, J., and Van Arsdale, R., 2004. Surficial Geologic Map of the Northwest Memphis Quadrangle, Shelby County, Tennessee, and Crittenden County, Arkansas, Scientific Investigations Map 2838, Version 1.0, U.S. Geological Survey.
- Clay, F.M., 1986. *A Century on the Mississippi: A History of the Memphis District U.S. Army Corps of Engineers 1876-1981*, U.S. Army Corps of Engineers, Memphis District.
- Cox, R., 2004. Surficial Geologic Map of the Northeast Memphis Quadrangle, Shelby County, Tennessee, Scientific Investigations Map 2839, Version 1.0, U.S. Geological Survey.
- Cramer, C.H., Gomberg, J.S., Schweig, E.S., Waldron, B.A., and Tucker, K., 2004. *The Memphis, Shelby County, Tennessee Seismic Hazard Maps*, U.S. Geological Survey Open-File Report 04-1294.
- Deutsch, C.V. and Journel, A.G., 1998. *GSLIB: Geostatistical Software Library and User's Guide*, 2nd Edition, Oxford University Press, New York, NY, 369 pp.
- Frankel, A.D., Petersen, M.D., Mueller, C.S., Haller, K.M., Wheeler, R.L., Leyendecker, E.V., Wesson, R.L., Harmsen, S.C., Cramer, C.H., Perkins, D.M., and Rukstales, K.S., 2002. *Documentation for the 2002 Update of the National Seismic Hazard Maps*, U.S. Geological Survey Open-File Report 02-420.
- Gomberg, J., 2004. personal communication.

- Holzer, T.L., Bennett, M.J., Noce, T.E., Padovani, A.C., and Tinsley, J.C. III, 2002. *Liquefaction Hazard and Shaking Amplification Maps of Alameda, Berkeley, Emeryville, Oakland, and Piedmont, California: a Digital Database*, U.S. Geological Survey Open-File Report 02-296.
- Holzer, T.L., Bennett, M.J., Noce, T.E., Padovani, A.C., and Tinsley, J.C. III, 2006a. *Liquefaction Hazard Mapping with LPI in the Greater Oakland, California Area, Earthquake Spectra*, in press.
- Holzer, T.L., Blair, J.L., Noce, T.E., and Bennett, M.J., 2006b. Predicted Liquefaction of East Bay Fills During a Repeat of a 1906 San Francisco Earthquake, *Earthquake Spectra*, in press.
- Holzer, T.L., Noce, T.E., Bennett, M.J., Tinsley, J.C. III, and Rosenberg, L.I., 2005. *Liquefaction at Oceano, California during the 2003 San Simeon Earthquake*, Bulletin of the Seismological Society of America, **95**, 2396-2411.
- Hwang, H., Chien, M.C., and Lin, Y.W., 1999. *Investigation of Soil Conditions in Memphis, Tennessee*, USGS Award No. 1434-HQ-98-GR-00002.
- Iwasaki, T., Tatsuoka, F., Tokida, K., and Yasuda, S., 1978. A practical method for assessing soil liquefaction potential based on case studies at various sites in Japan, in *Proceedings 2nd International Conference on Microzonation*, pp. 885-896.
- Iwasaki, T., Tokida, K., Tatsuoka, F., Watanabe, S., Yasuda, S., and Sato, H., 1982. Microzonation for soil liquefaction potential using simplified methods, in *Proceedings 3rd International Conference on Microzonation*, pp. 1319-1330.
- Liao, T., Mayne, P.W., Tuttle, M.P., Schweig, E.S., and Van Arsdale, R.B., 2002, CPT site characterization for seismic hazards in the New Madrid seismic zone, *Engineering Geology*, **22**, 943-950.
- Liao, T., Zavala, G., McGillivray, A., Camp, W.M., III, and Mayne, P.W., 2001. Cone Penetration Testing for Seismic Hazards Evaluation in Memphis & Shelby County, Tennessee. USGS Grant 00HQGR0025 Final Report. 17 pp.
- Lin, H., Hwang, H.H.M., and Chou, T., 1996. *Estimation of Liquefaction Potential and Permanent Ground Deformation Using Neural Network Technology and GIS*, Center for Earthquake Research and Information, The University of Memphis.
- Luna, R., and Frost, J.D., 1998. A spatial liquefaction analysis system, *Journal of Computing in Civil Engineering*, **12**(1), 48-56.
- Moore, D.W., and Diehl, S.F., 2004a. Surficial Geologic Map of the Southeast Memphis Quadrangle, Shelby County, Tennessee, Scientific Investigations Map 2822, Version 1.0, U.S. Geological Survey.

- Moore, D.W., and Diehl, S.F., 2004b. Surficial Geologic Map of the Southwest Memphis Quadrangle, Shelby County, Tennessee, and Crittenden County, Arkansas, Scientific Investigations Map 2823, Version 1.0, U.S. Geological Survey.
- Ng, K.W., Chang, T.S., Hwang, H.H.M., 1989. *Surface conditions of Memphis and Shelby County*, Technical Report NCEER-89-0021.
- Obermeier, S.F., 1989. *The New Madrid Earthquakes: An Engineering-Geologic Interpretation of Relict Liquefaction Features*, U.S. Geological Survey Professional Paper 1336-B.
- Robertson, P.K., 1990. Soil classification using the cone penetration test, *Canadian Geotechnical Journal*, **27**, 151-159.
- Seed, H.B. and Idriss, I.M., 1971. Simplified procedure for evaluating soil liquefaction potential, *Journal of the Soil Mechanics and Foundations Division* **97**, 1249-1273.
- Toprak, S. and Holzer, T.L., 2003. Liquefaction potential index: field assessment, *Journal of Geotechnical and Geoenvironmental Engineering*, **129**(4), 315-322.
- Tuttle, M.P., Schweig, E.S., Sims, J.D., Lafferty, R.H., Wolf, L.W., and Haynes, M.L., 2002. The Earthquake Potential of the New Madrid Seismic Zone, *Bulletin of the Seismological Society of America* **92**, pp. 2080-2089.
- Van Arsdale, R., 2004a. Surficial Geologic Map of the Ellendale Quadrangle, Shelby County, Tennessee, Scientific Investigations Map 2836, Version 1.0, U.S. Geological Survey.
- Van Arsdale, R., 2004b. Surficial Geologic Map of the Germantown Quadrangle, Shelby County, Tennessee, Scientific Investigations Map 2837, Version 1.0, U.S. Geological Survey.
- Van Arsdale, R.B. and Cox, R., 2003. *Surficial Geologic and Liquefaction Susceptibility Mapping in Shelby County, Tennessee*, USGS Award No. 00HQGR0031.
- Wheeler, R.L. and Perkins, D.M., 2000. *Research, Methodology, and Applications of Probabilistic Seismic Hazard Mapping of the Central and Eastern United States- Minutes of a Workshop on June 13-14, 2000, at Saint Louis University*, U.S. Geological Survey Open File Report 00-0390.
- Yates, R., Waldron, B., and Van Arsdale, R. 2003. Urban effects on flood plain natural hazards: Wolf River, Tennessee, USA, *Engineering Geology*, **70**, 1-15.
- Youd, T.L. and Perkins, D.M., 1978. Mapping liquefaction-induced ground failure potential, *Journal of the Geotechnical Engineering Division* **104**, 433-446.
- Youd, T.L., Idriss, I.M., Andrus, R.D., Arango, I., Castro, G., Christian, J.T., Dobry, R., Finn, W.D.L., Harder, L.F. Jr., Hynes, M.E., Ishihara, K., Koester, J.P., Liao, S.S.C., Marcuson, W.F. III, Martin, G.R., Mitchell, J.K., Moriwaki, Y., Power, M.S., Robertson, P.K., Seed, R.B., and Stokoe, K.H. II, 2001. Liquefaction resistance of soils: summary report from the 1996 NCEER

and 1998 NCEER/NSF workshop on evaluation of liquefaction resistance of soils, *Journal of Geotechnical and Geoenvironmental Engineering* **127**, 817-833.

Table 1. Surficial geology of the Memphis/Shelby County, Tennessee area (Van Arsdale and Cox, 2003).

Surficial Geology	Description
Qal	Holocene alluvium; sand, clayey silt, and minor gravel; sand is very fine to coarse grained quartz with chert; thick-bedded basal point bar sands are overlain by alternating thin beds of sand and silt and capped by overbank clayey silt.
Qa	Holocene alluvium; silt with minor mixed sand and clay; dispersed sand is very fine to very coarse grained quartz and minor chert; floodplain of Nonconnah Creek and tributaries to Wolf River and Nonconnah Creek consist of reworked loess; channel bars are covered with sand and gravel.
Ql	Late Pleistocene loess; silt with < 10 percent sand and < 10 percent clay; loess is dominantly quartz; thickness ranges from 2 to 20 m.
Qtl	Pleistocene loess-covered terrace; dense, cross-bedded, medium-grained sand capped by loess silt.
Artificial Fill (af)	Holocene, man-made; mostly silt, sand, and chert gravel locally derived from loess, alluvium, and the Lafayette gravel.

Table 2. Number of SPT and CPT profiles in each geologic unit.

Geologic Unit	Number of SPT Profiles	Number of CPT Profiles
Qal	104	0
Qa	113	12
Ql	370	4
Qtl	36	2
Total	623	18

Table 3. Assumed fines content based on USCS soil type.

USCS Soil Type	Assumed Fines Content (%)
GW, GP, SW, SP	0
GW-GM, GW-GC, GP-GM, GP-GC, SW-SM, SW-SC, SP-SM, SP-SC	5
GC, GM, GC-GM, SC, SM, SC-SM	12

Table 4. Categories for SPT profiles based on completeness of data.

Category	SPT Profile	USCS Classification	Number of Profiles
1	Complete to 20 m	Complete to 20 m	122
2	Complete to 18 m	Complete to 18 m	153
3	Complete to 15 m	Complete to 15 m	68
4	Complete to 20 m	Incomplete	206
5	Complete to 18 m	Incomplete	28
6	Complete to 15 m	Incomplete	148

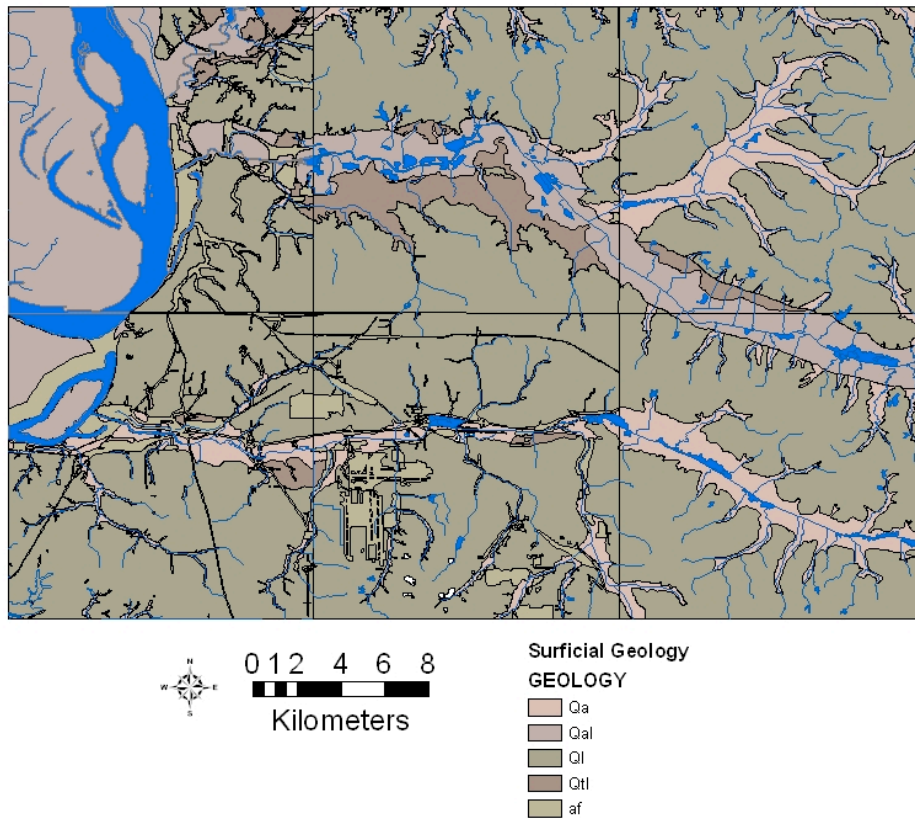
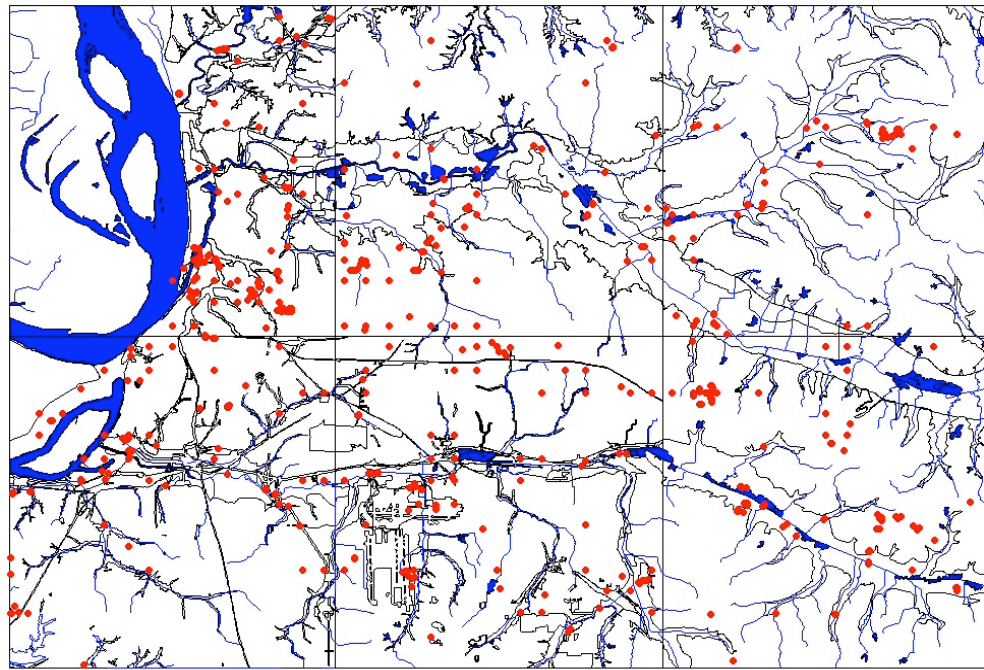
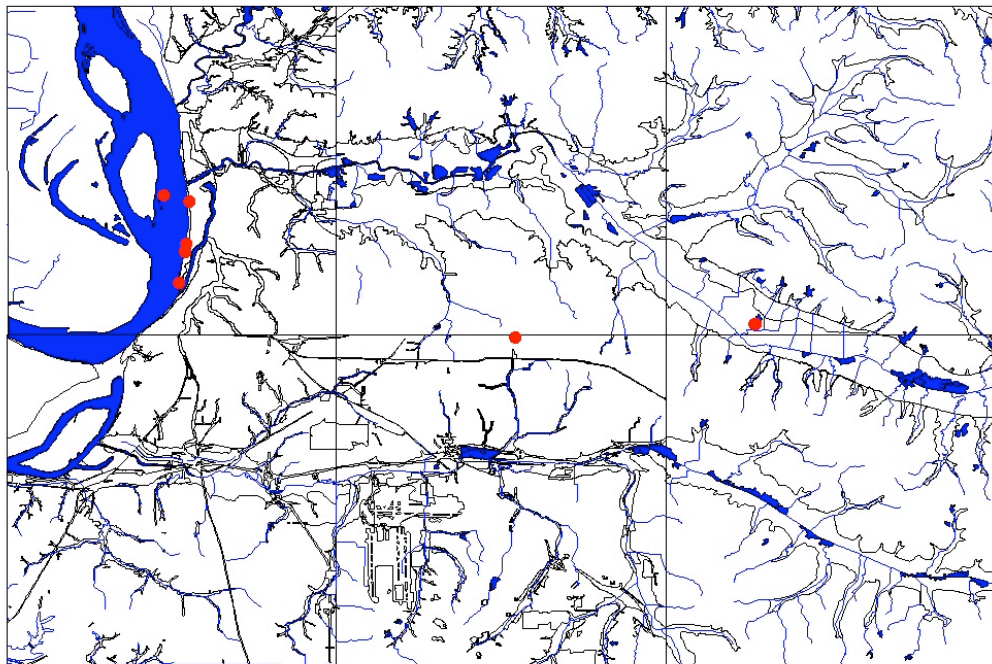


Figure 1. Surface Geology of Memphis/Shelby County, Tennessee (Broughton and Van Arsdale, 2004; Cox, 2004, Moore and Diehl, 2004a; 2004b; Van Arsdale, 2004a; 2004b)



● SPT data
 ■ Water

5 0 5 10 Kilometers



● CPT data
 ■ Water

5 0 5 10 Kilometers



Figure 2. Location of (a) SPT and (b) CPT profiles

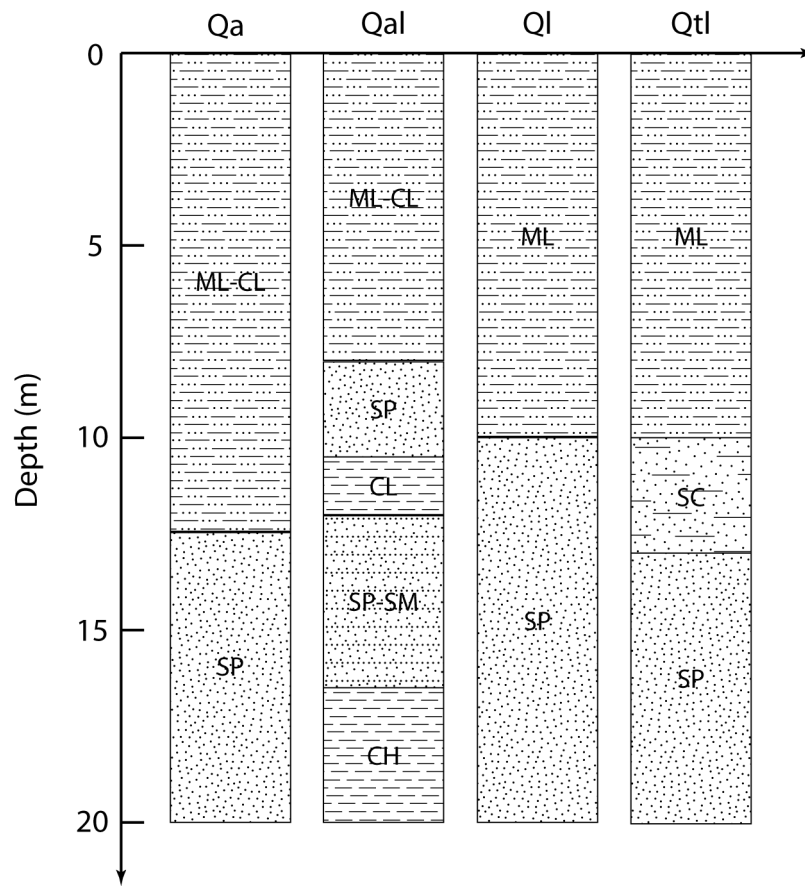


Figure 3. Representative Soil Profiles for Each Geologic Unit

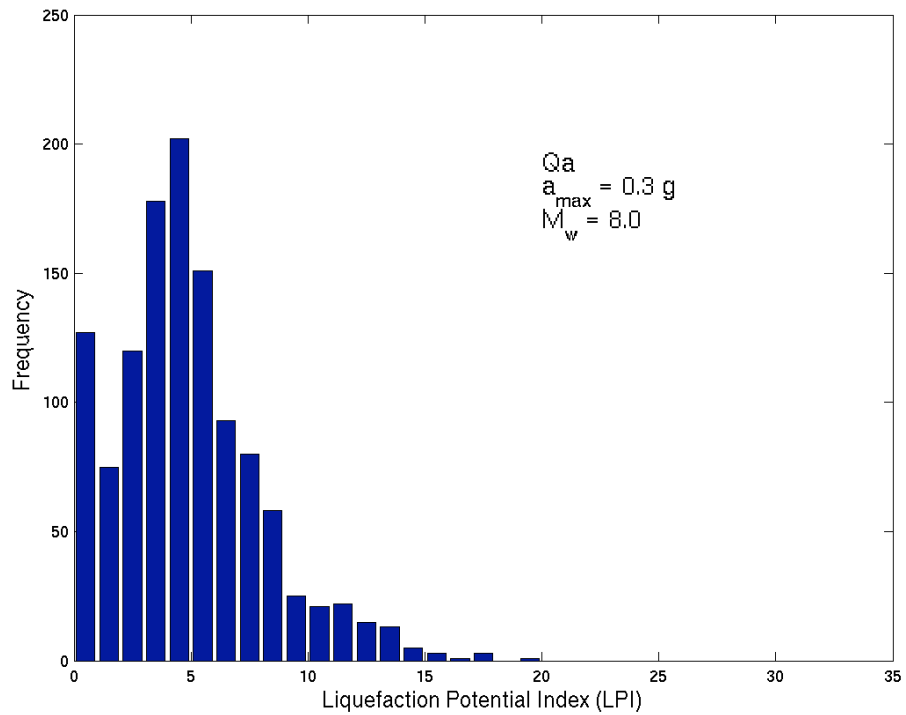
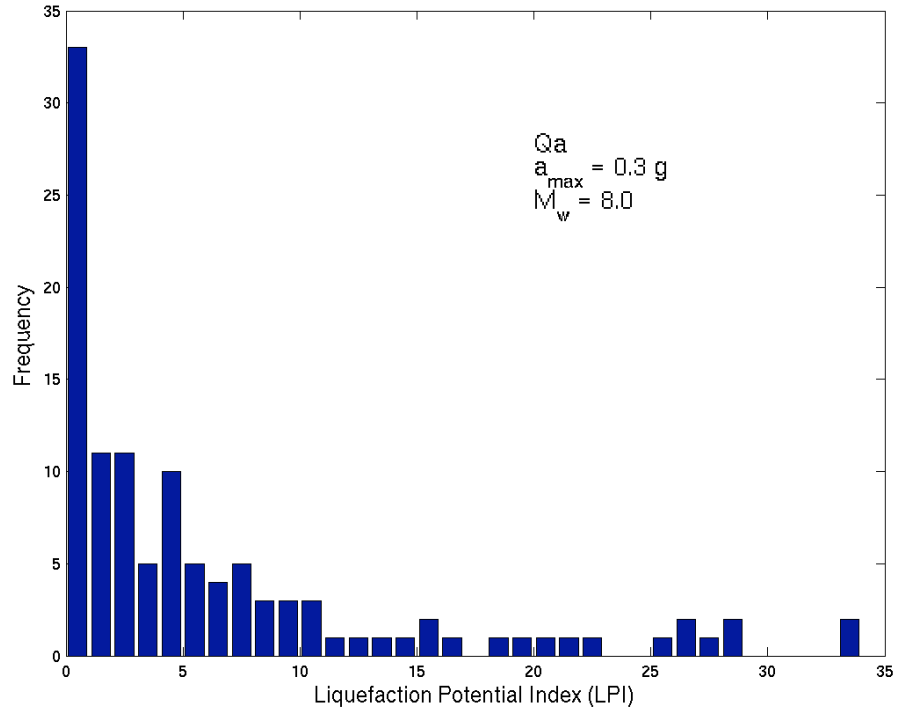


Figure 4. Histogram of LPI for (a) SPT data and (b) CPT data for Unit Qa, $a_{\max} = 0.3 \text{ g}$, and $M_w = 8.0$

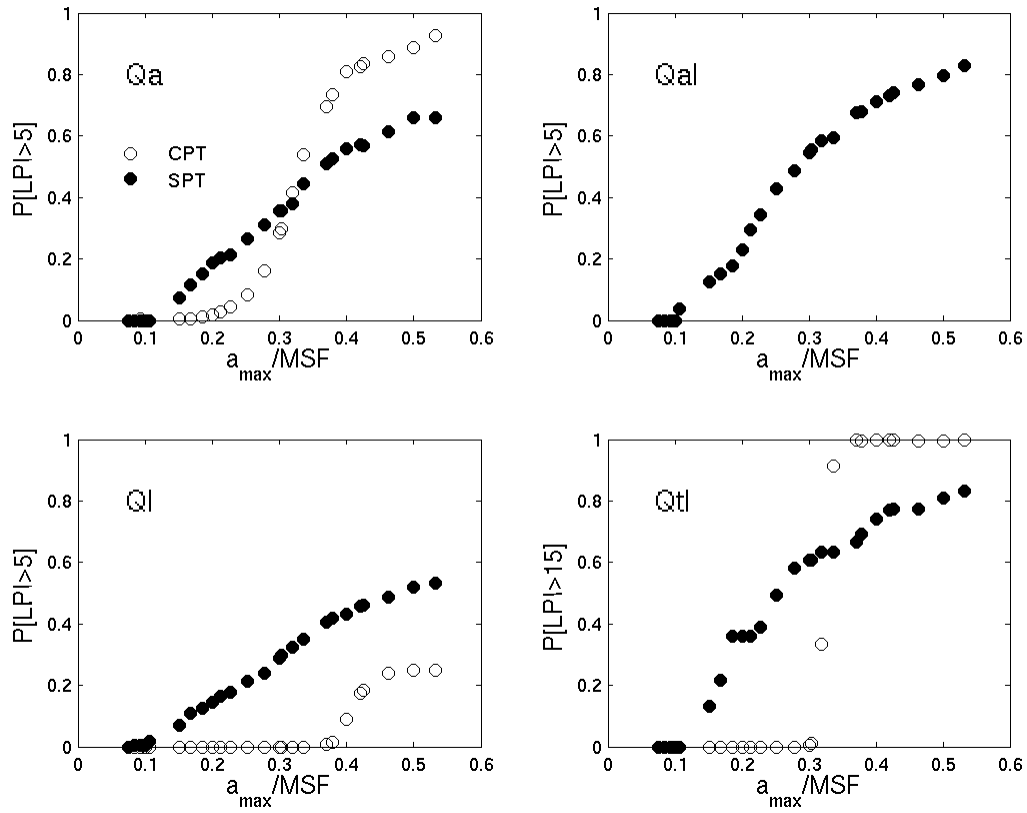


Figure 5. Probability of LPI > 5 for each Geologic Unit

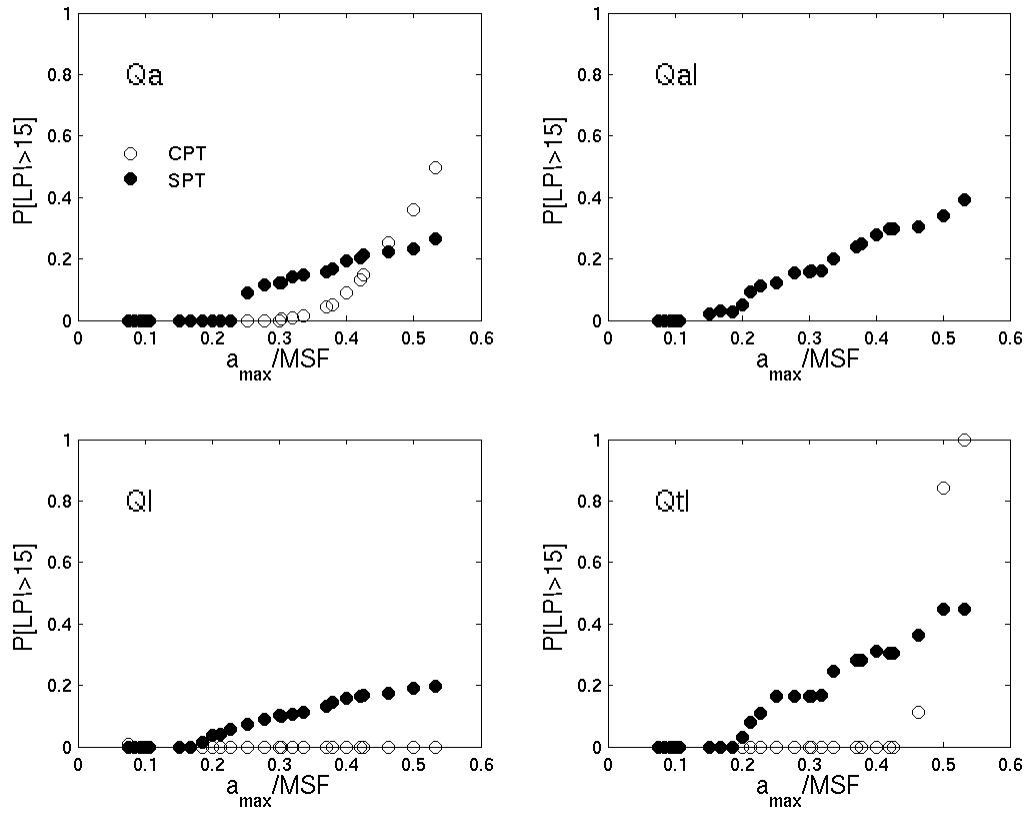


Figure 6. Probability of LPI > 15 for each Geologic Unit

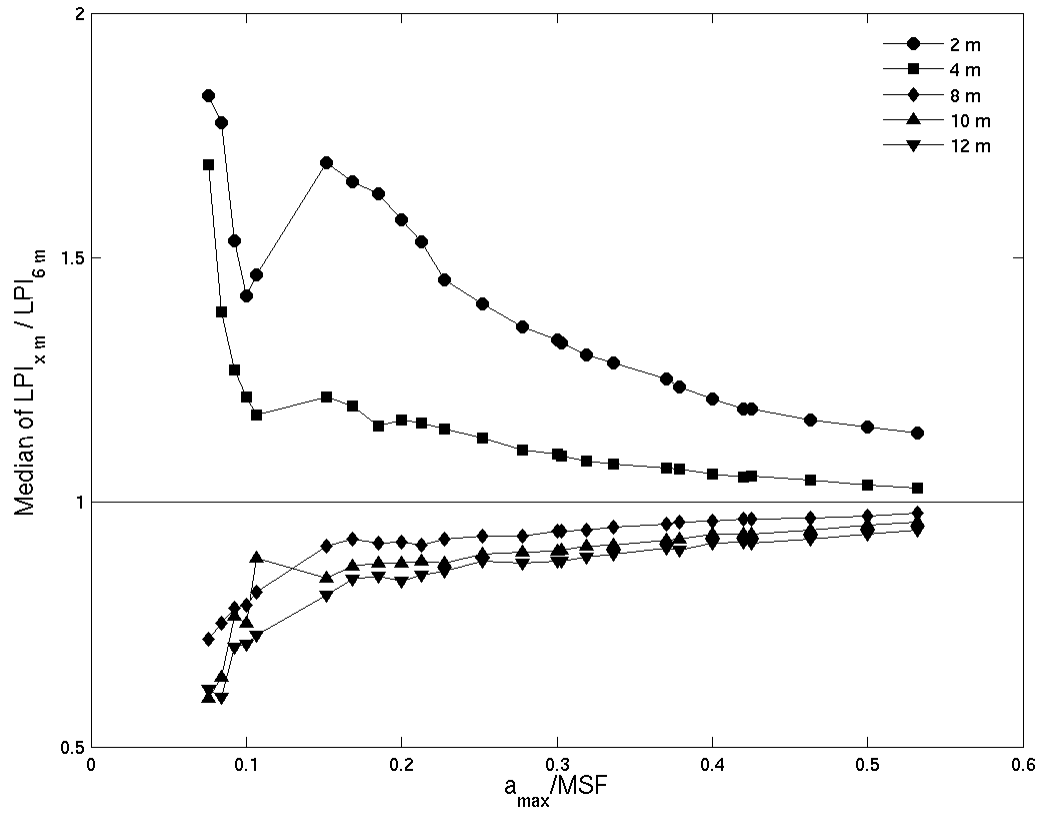


Figure 7. Effect of Assumed Groundwater Table Depth on LPI Calculations

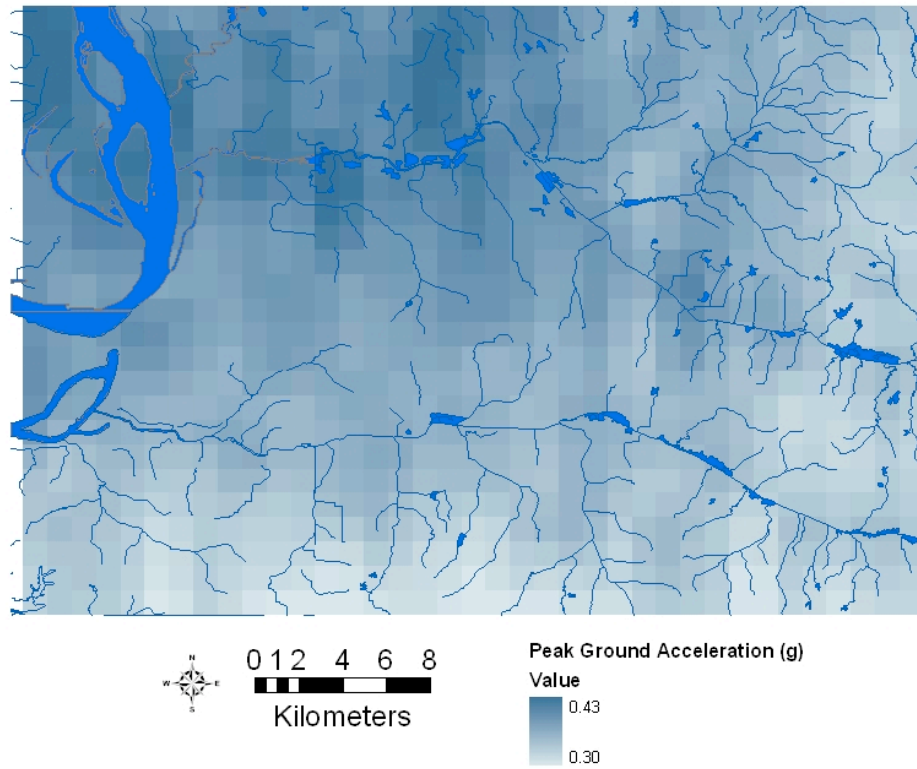


Figure 8. Peak Ground Acceleration in the Study Area due to a $M_w = 7.7$ Scenario Earthquake (based on Cramer et al., 2004)

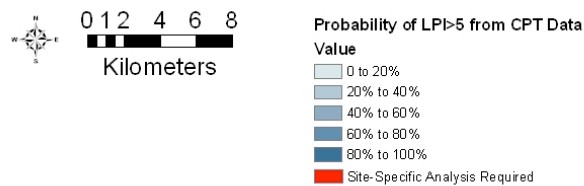
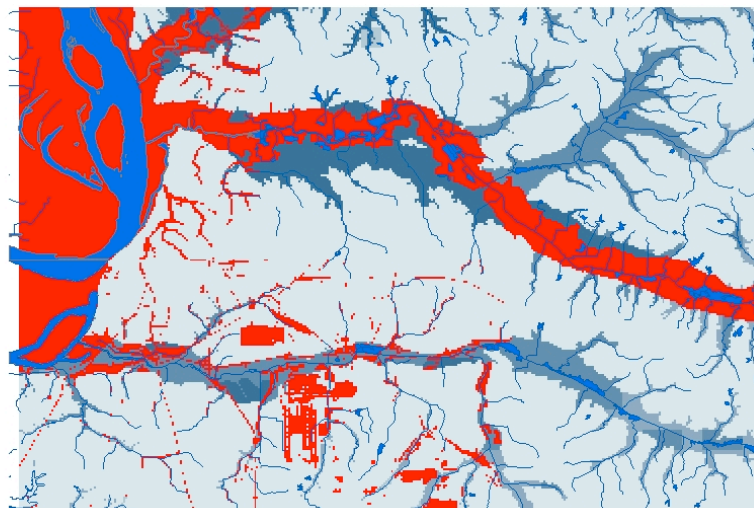
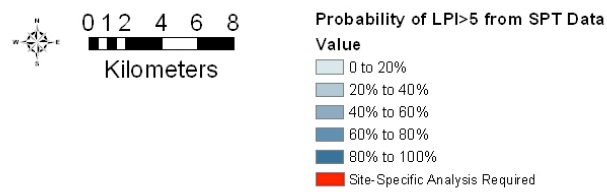
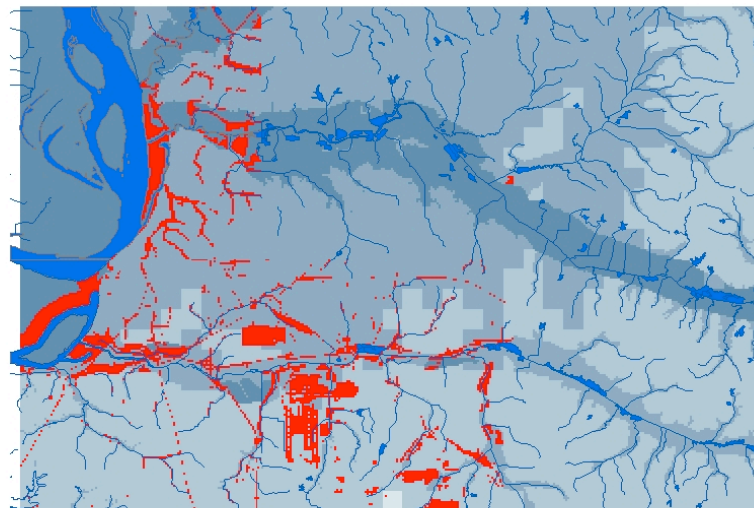


Figure 9. Probability of Moderate Liquefaction ($LPI > 5$) in the Study Area due to a $M_w = 7.7$ Scenario Earthquake from (a) SPT and (b) CPT data

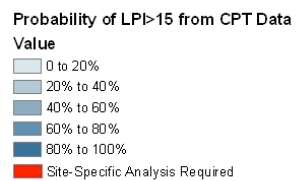
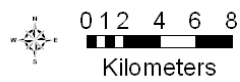
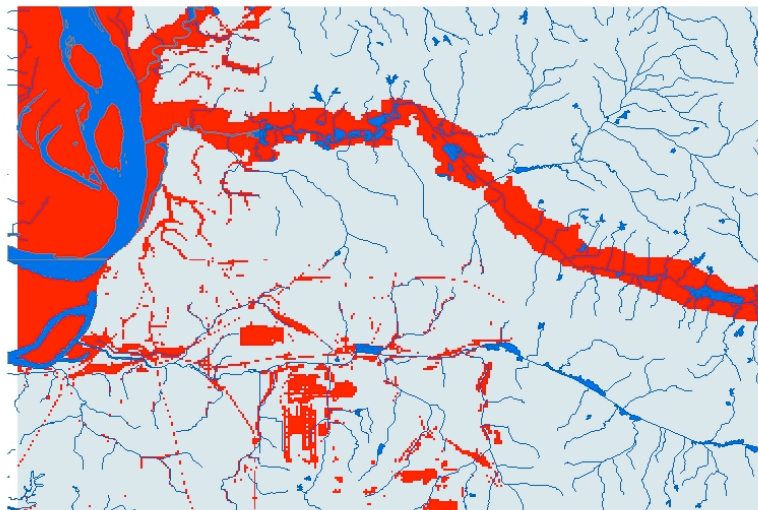
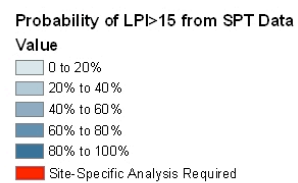
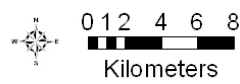
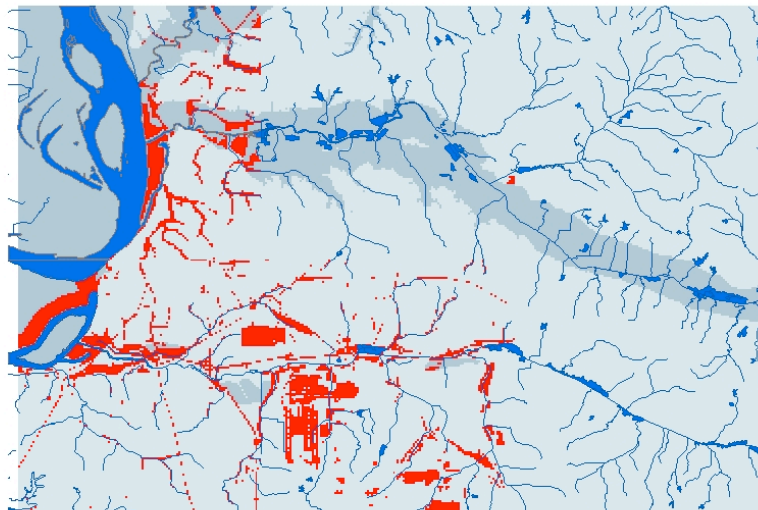


Figure 10. Probability of Major Liquefaction (LPI > 15) in the Study Area due to a $M_w = 7.7$ Scenario Earthquake from (a) SPT and (b) CPT data

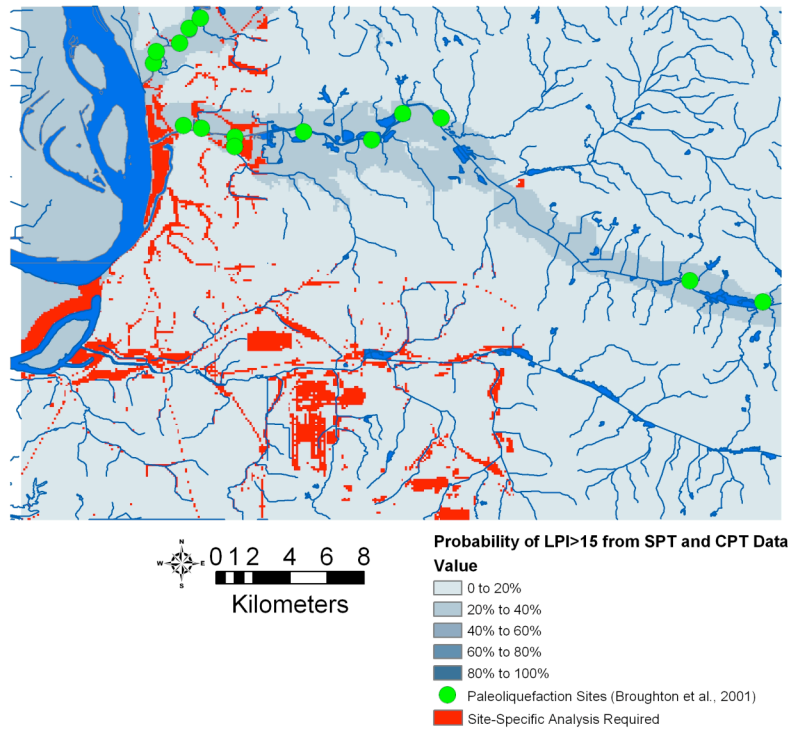
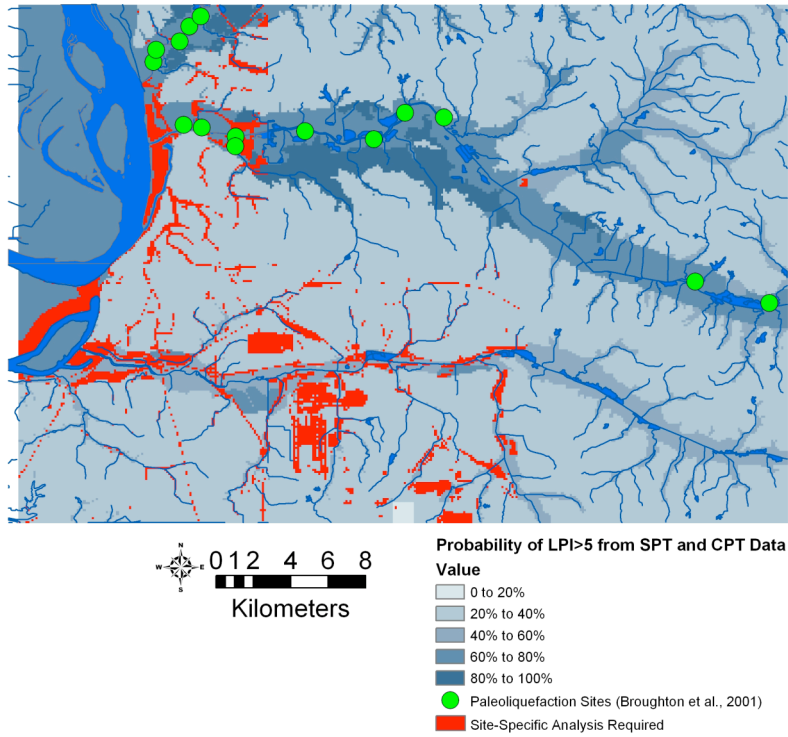


Figure 11. Probability of (a) Moderate (LPI > 5) and (b) Major (LPI > 15) Liquefaction in the Study Area due to a $M_w = 7.7$ Scenario Earthquake from Combined SPT and CPT data and Comparison with Paleoliquefaction Features